EFFECTS OF LAMELLAR BOUNDARIES ON CREEP BEHAVIOR OF PST CRYSTALS OF TiAl ALLOYS①

Lin Jianguo, Zhang Yonggang and Chen Changqi
Department of Materials Science and Engineering,
Beijing University of Aeronautics and Astronautics, Beijing 100083, P. R. China

ABSTRACT TiAl PST crystals were grown using an induction floating zone melting furnace. The creep behavior and deformation structure at 800 ℃ were studied for the samples with three orientations. The results indicate that the creep behavior of PST crystals is strongly dependent on the lamellar orientation with respect to the loading axis. The presence of lamellar boundaries influences the creep deformation. They may not only inhibit shear deformation across the lamellae, but also pin the dislocation and restrict its motion.

Key words TiAl alloy PST crystal creep behavior deformation twin

1 INTRODUCTION

Without a fundamental understanding of its creep behavior, there is great risk associated with the use of TiAl in the envisaged critical propulsion applications. Recent investigations have shown that the creep strength of TiAl alloys is very sensitive to microstructure, and the microstructure with fully lamellar structure has been found to have the highest creep resistance[1,2]. Those are associated with the lamellar boundaries[3,4]. However, there have been only a limited number of studies dealing with the creep mechanism, especially the effects of lamellar boundaries on creep of this fully lamellar structure. Polysynthetically twinned (PST) crystal provides a good simulating material for studying the mechanism of creep in the alloys with fully lamellar structure, because the so-called PST crystals contains a single set of lamellar structure. In this study, PST crystals were grown and their creep behavior was investigated, focusing on the effects of lamellar boundaries on creep deformation.

2 EXPERIMENTAL PROCEDURE

Ti-48Al (mole fraction, %) PST crystal rods with a diameter of 8 mm were grown using an induction floating zone furnace. The compression specimens with the dimension of 3 mm × 3 mm × 6 mm were cut from as-grown PST crystal, as schematically shown in Fig. 1. The angle between lamellar boundary and compression axis was represented by ϕ. The compression creep behavior of the samples with three orientations, i.e., ϕ= 0°, 45° and 90°, was studied in this paper. Compression creep testing was conducted at 800 ℃ in air under constant load on a compression creep test machine. The stress levels were 150 MPa for the samples with ϕ= 45° and 350 MPa for ϕ= 0° and 90° respectively. The TEM observations of the deformation structure at the secondary stage for the three oriented samples were carried out on a Hitachi H-800 transmission electron microscope.

3 RESULTS

3.1 Creep curves for samples with three orientations

The creep curves for the samples with ϕ= 45°, 0° and 90° at 800 ℃ and stress level of 150 MPa and 350 MPa are shown in Fig. 2, as strain vs time (εt) plots. As can been seen, for the samples with ϕ= 45°, the creep curve exhibits a

① Received Nov. 27, 1997; accepted Apr. 17, 1998

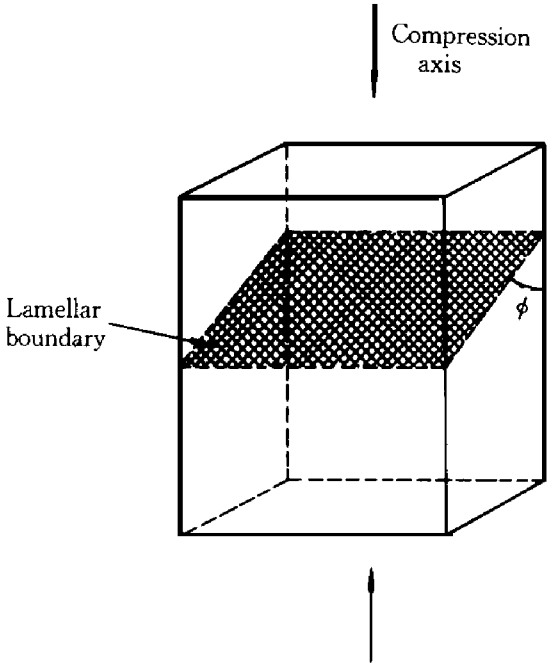

Fig. 1 Geometry of compression sample

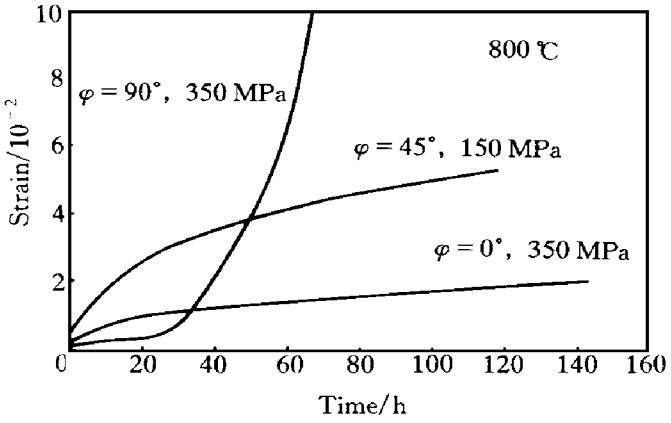

Fig. 2 Creep curves (εt) of TiAl PST crystal samples with three orientations at 800 ℃

pronounced primary creep regime at a lower stress level in comparison with the two other orientations. The strain at the minimum creep rate is about 3%, and the minimum strain rate is $2.39 \times 10^{-4}\ h^{-1}$ at $\sigma = 150$ MPa, while for the samples with $\phi = 0°$ and 90°, although at a much higher stress level than that for the sample with $\phi = 45°$, i. e., 350 MPa, the primary strain is much smaller, especially for the sample with $\phi = 90°$. Therefore, in comparison with the samples with hard orientations (i. e., $\phi = 0°$ and 90°), the creep resistance for the samples with $\phi = 45°$ is much lower.

It is interesting to note that, under 350 MPa stress level, the tertiary creep stage for the samples with $\phi = 90°$ is early onset, although this oriented sample exhibits the highest strength among the three oriented samples[6].

3.2 Observation of deformation structure at secondary stage

TEM observation and analysis show that, for the samples with $\phi = 45°$, the creep deformation occurs primarily by the activation of normal dislocations with $\boldsymbol{b} = 1/2\langle 110]$, and the motion of these dislocations is parallel to lamellar boundaries. Therefore, no direct interaction of the dislocations and lamellar boundaries is found in these oriented samples. In some lamellae, it can be noted that dislocations are trapped in interface boundaries and bowing between them, as shown in Fig. 3, which indicates that the boundary in-

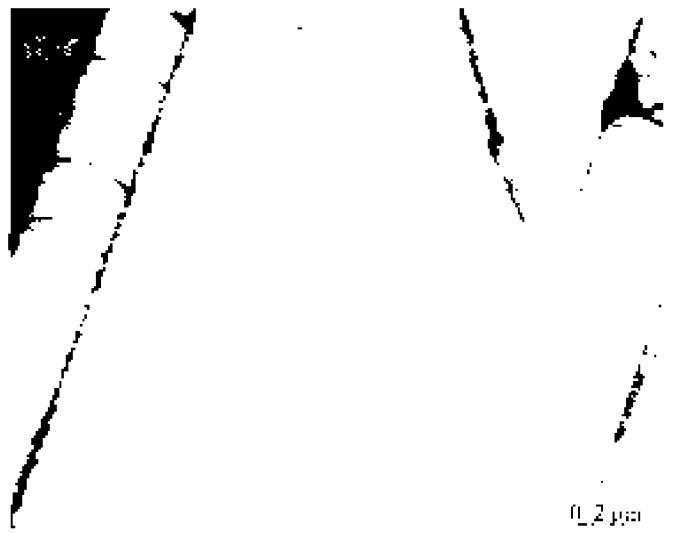

Fig. 3 TEM micrograph of deformation structure for sample with $\phi = 45°$ crept at 800 ℃, showing that dislocatons were pinned at boundaries and bowed ($\varepsilon \approx 4\%$)

terfaces can pin the dislocation. In comparison with the samples with $\phi = 45°$, the creep deformation structures in the samples with $\phi = 0°$ and 90° are quite different. Dislocations with $\boldsymbol{b} = 1/2\langle 110]$ and deformation twins of $\{111\}\ 1/6\langle 112]$ type are observed to be activated on the $\{111\}$ planes across lamellar boundaries, and the propagation of shear deformation (mainly twinning) is

hindered by the lamellar boundaries. Figs. 4(a), (b) and (c) exhibit the interaction between deformation and lamellar boundaries in the crept samples with $\phi = 90°$ ($t = 800$ ℃, $\varepsilon \approx 4\%$; TT, RT and PT denote true-twin type, 120° rotational type and pseudo-twin type boundaries, respectively). When a deformation twin encounters a true-twin type boundary, it can enter the barrier lamella and the deformation twins may pass through a series of true-twin type lamella in a zigzag mode, as shown in Fig. 4(a). When a deformation twin encounters the 120° rotational type lamellar boundary, it is stopped at the boundary, and deformation mode changes from twinning to slip on the propagation of shear deformation across such domain boundaries, as shown in Fig. 4(b). Contrast analysis indicates that these dislocations are normal dislocations with $\boldsymbol{b} = 1/2\langle 110]$, and slip on the planes parallel to the twinning planes. However, when the deformation twins encounter the pseudo-twin type lamellar boundaries and α_2/γ interfaces, they are stopped at these boundaries, as shown in Figs. 4(a) and (c).

4 DISCUSSION

The microstructure of PST crystals is characterized with a large number of boundary interfaces. It is well documented that, because the direction and the other two directions on the (111) plane in the TiAl phase with $L1_0$ structure are not equivalent to each other, while three directions on the basal plane in the Ti_3Al phase with the hexagonal $D0_{19}$ are all equivalent, there exist six types of ordered domains in PST crystals, which are called six variants[5]. Thus, three types of lamellar boundaries can be formed between two neighbor variants, i.e., true-twin type boundary, 120°-rotational type boundary and pseudo-twin type boundary. The crystallographic relationship between two neighbor domains at these three types of boundaries can be represented by the Thomson tetrahedron, as shown in Fig. 5.

As expected that the strong anisotropy in compression creep behavior was identified in TiAl PST crystals. It is attributed to the defor-

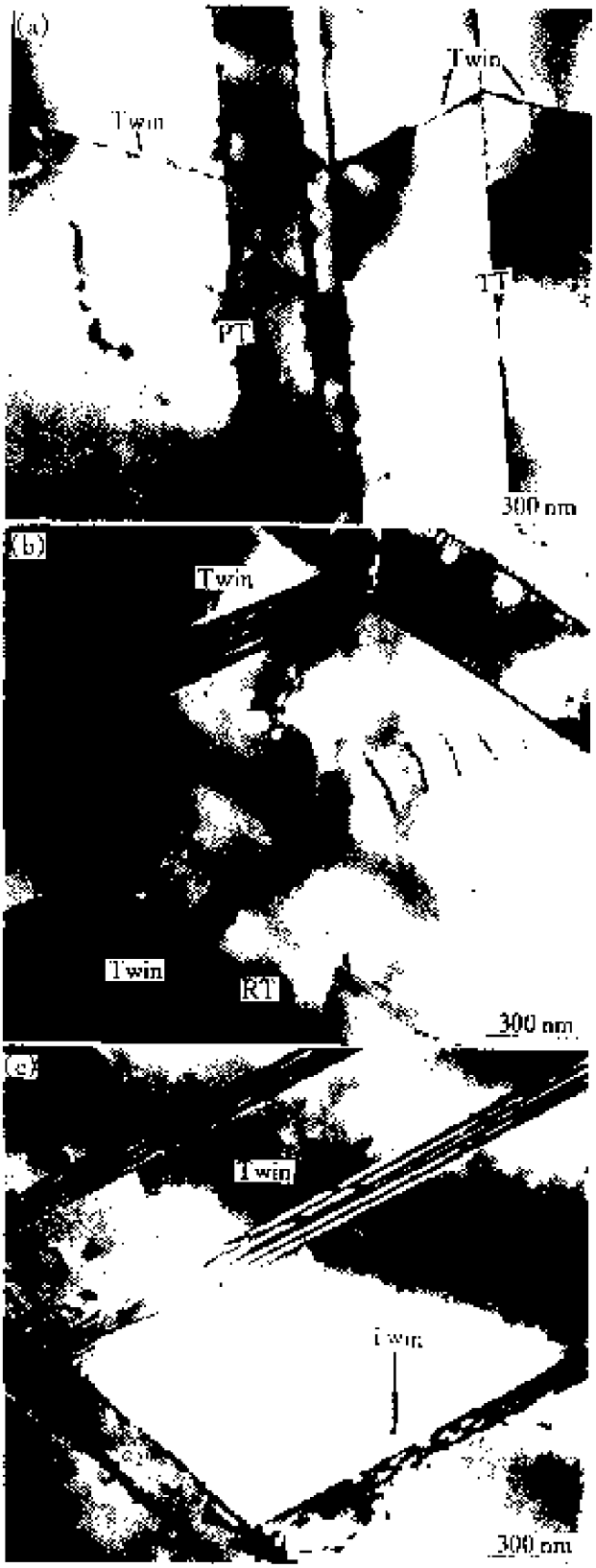

Fig. 4 TEM micrographs of deformation structure with $\phi = 90°$ showing interaction between twinning and different lamellar boundaries (a) —Interaction between twinning and true-twin type and pseudo-twin type boundaries; (b) —Interaction between twinning and 120° rotational type boundary; (c) —Interaction between twinning and α_2/γ interface

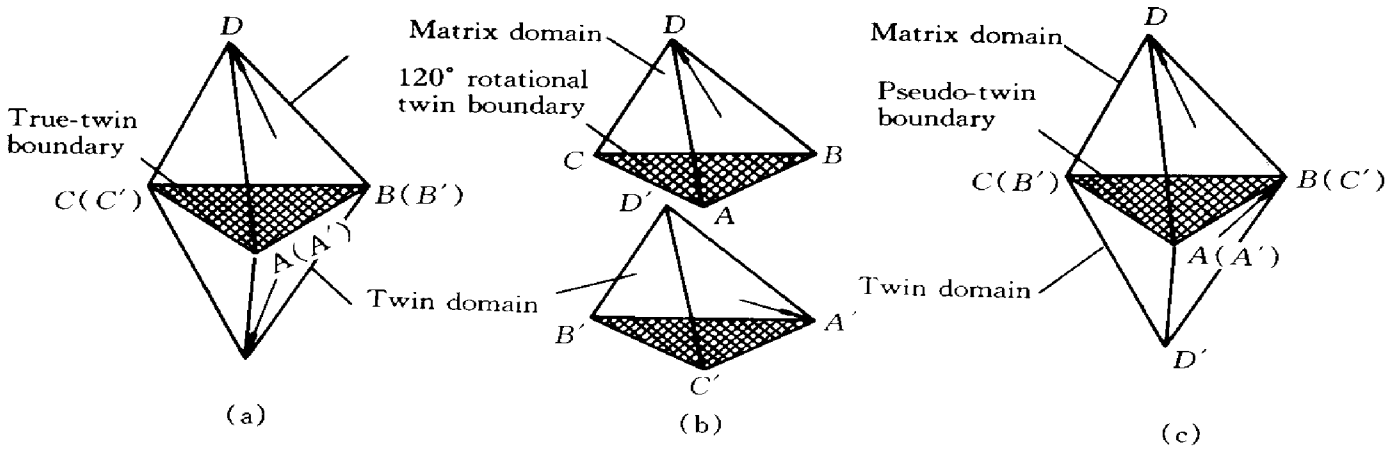

Fig. 5 Crystallographic relationship between two neighbor γ lamellae represented by Thompson tetrahedron (The arrows show the twinning direction)

mation mode of PST crystals with different orientations. When the angle between the loading axis and lamellar boundaries is 45°, i. e., ϕ= 45°, the slip systems on the {111} planes parallel to the lamellar boundaries are activated firstly due to high shear stress, so the shear deformation in these oriented samples is mainly parallel to the lamellar boundaries. As a result, these oriented samples exhibit low yield strength and creep resistance. On the other hand, when the load is applied parallel or normal to the lamellar boundaries, i. e., ϕ= 0° or 90°, shear deformation only occurs on the {111} planes across lamellar boundaries, then the dislocations and deformation twin will interact with the lamellar boundaries. TEM examination reveals that the lamellar boundaries can effectively inhibit the dislocations and deformation twins crossing them, so the fine interface spacing reduces the glide distance. Consequently, the samples with ϕ= 0° and 90° exhibit much higher yield strength and creep resistance than that of samples with ϕ= 45°. However, for the samples with ϕ= 90°, the tertiary creep regime surprisingly starts much earlier than those for the two other oriented samples do, which may be associated with the spheroidization of α_2 during the creep[6]. When the stress is applied perpendicular to the lamellar boundaries, only the pyramidal slip (i. e., $\{1\bar{1}21\}\langle 11\bar{2}6\rangle$) can be activated, for which the resolved shear stress is much higher than that for prismatic slip (i. e., $\{\bar{1}100\}\langle 11\bar{2}0\rangle$) which can be activated when the stress is applied parallel to the lamellar boundaries[7]. Thus, when the deformation occurs across the lamellar planes, a high stress concentration will be built up at the γ/α_2 boundaries, which may cause α_2 plates to be split and spheroidization. It causes the creep instability of the samples with ϕ = 90°.

The anisotropy of creep resistance and creep deformation structure of PST crystals indicate that the boundary interfaces can inhibit dislocation and deformation twin motion, leading to improved creep resistance. Two mechanism have been suggested to account for this improvement as follows.

First, boundary interfaces in PST crystals can inhibit the shear deformation across the lamellae. The observation of the interaction between deformation twinning and lamellar boundaries reveals that the mechanisms in which three types of lamellar boundaries inhibit the propagation of twinning are quite different, which can be explained in the view of crystallographical relationship between the two neighbor domains. It can be seen that the relevant slip systems in the two neighbor domains are in mirror symmetry about the true-twin type boundary, as seen in Fig. 5(a). Thus, when a deformation twinning encounters this type boundary, the true-twin type domain may accommodate the twining shear

by secondary twinning on the mirror plane, and the propagation of twinning becomes more difficult due to the change of twinning plane and direction. For the 120° rotational type boundary, since the twinning plane are continuously distributed across the domain boundaries but the twinning shear is rotated 120°, as shown in Fig. 5(b), the twinning shear can be accommodated into the barrier domain by the activation of the dislocations with $\boldsymbol{b}=1/2\langle 110]$ on the continuous {111} plane. While, for the pseudo-twin type boundary, the twinning plane is not only deflected but also rotated across the boundary, as seen in Fig. 5(c). Therefore, the twinning shear is hard to be transferred across such a boundary. Since the interface is discontinuous both in chemical composition and crystal structure, propagation of a twinning shear across such an interface would not be expected to be easy. On the basis of the experimental observations and analysis, it can be noted that the pseudo-twin type of boundary and the interface are effective barriers to the propagation of deformation twin.

Second, the boundary interfaces can pin the dislocations to restrict dislocation motion, causing bowing of dislocation between interfaces. This mechanism is similar to the interaction of dislocations with the dispersed particles when a dislocation passes the particles by the looping mechanism. A shear stress, τ_0, is required to cause the dislocation bowing out from the pinning points, which can be calculated according to Orowan equation, i.e.,

$$\tau_0 = \frac{Gb}{2\pi L}\ln\frac{L}{2b} \qquad (1)$$

where G is shear modulus, b is Burgers vector and L is lamellar interface spacing. It is suggested that, for TiAl alloys, the fully lamellar microstructure with fine lamellar interface spacing is expected to exhibit a much higher creep resistance.

5 CONCLUSIONS

(1) The strong anisotropy in creep behavior was identified in TiAl PST crystals. The creep resistance of samples with $\phi = 0°$ and 90° is much higher than that of samples with $\phi = 45°$.

(2) The presence of lamellar boundaries has an important influence on the creep deformation. They may not only inhibit shear deformation across the lamellae, but also pin the dislocations and restrict their motion.

(3) Among the four types of lamellar interfaces in PST crystals, the pseudo-twin type boundary and α_2/γ interface are effective barriers to the propagation of deformation twin.

REFERENCES

1 Worth D, John J W and Allison J E. In: Kim Y W, Wagner R and Yamaguchi M eds. Gamma Titanium Aluminide. Las Vegas: The Minerals, Metals and Materials Society, 1995: 931.

2 Beddoes J, Zhao L, Au P *et al*. In: Nathal M V, Darolia R, Liu C T *et al* eds. Structural Intermetallics 1997. Champion, PA: The Minerals, Metals and Materials Society, 1997: 109.

3 Beddoes J, Wallace and Zhao L. Int Mater Rev, 1995, 40(5): 197.

4 Hsung L M and Niel T G. In: Nathal M V, Darolia R, Liu C T *et al* eds. Structural Intermetallics 1997. Champion, PA: The Minerals, Metals and Materials Society, 1997: 129.

5 Lin Jianguo, Zhou Yajian, Zhang Yonggang *et al*. Rare Metal Materials and Engineering, (in Chinese), 1996, 25(2): 21.

6 Lin Jianguo. PhD Dissertation, (in Chinese). Beijing: Beijing University of Aeronautics and Astronautics, 1996: 121.

7 Inui H, Oh M H, Nakamura A. Acta Metall Mater, 1992, 40(11): 2039.

8 Wang J N, Schwartz A J, Niel T G *et al*. In: Kim Y W, Wagner R and Yamaguchi M eds. Gamma Titanium Aluminide. Las Vegas: The Minerals, Metals and Materials Society, 1995: 949.

(Edited by Peng Chaoqun)